

## Dissolution of a Liquid Microdroplet in a Nonideal Liquid-Liquid Mixture Far from Thermodynamic Equilibrium

Pietro Poesio,<sup>1,\*</sup> Gian Paolo Beretta,<sup>1</sup> and Todd Thorsen<sup>2</sup>

<sup>1</sup>Università degli Studi di Brescia, via Branze 38, 25123 Brescia, Italy

<sup>2</sup>Massachusetts Institute of Technology, Cambridge, Massachusetts 02139-4307

(Received 6 December 2008; published 5 August 2009)

A droplet placed in a liquid-liquid solution is expected to grow, or shrink, in time as  $\sim t^{1/2}$ . In this Letter, we report experimental evidence that when the composition in the interface is far from thermodynamic equilibrium due to the nonideality of the mixture, a droplet shrinks as  $\sim t$ . This scaling is due to the coupling between mass and momentum transfer known as Korteweg forces as a result of which the droplet self-propels around. The consequent hydrodynamic convection greatly enhances the mass transfer between the droplet and the bulk phase. Thus, the combined effect of nonideality and nonequilibrium modifies the dynamical behavior of the dissolving droplet.

DOI: 10.1103/PhysRevLett.103.064501

PACS numbers: 47.51.+a, 64.75.Bc, 68.05.-n

The formation and dissolution of gas bubbles and liquid droplets in liquid-gas and liquid-liquid systems are major concerns in many industrial processes as they occur in mixing and separation, in dispersion of food products, and in pharmaceutically controlled drug delivery, for instance. When a gas bubble or a liquid droplet is placed in a gas-liquid or liquid-liquid mixture, it is expected to grow (or to shrink) by diffusion; this process is described by the well-known diffusion equation, as  $\partial\phi_1/\partial t = -\nabla \cdot \mathbf{j}_1$  in terms of the local concentration  $\phi_1(\mathbf{r}, t)$  and mass flux  $\mathbf{j}_1$  of component  $A$  in the mixture. If one assumes a binary, ideal mixture, the net mass flux can be calculated by Fick's law,  $\mathbf{j}_1 = -D_0\nabla\phi_1$ , where  $D_0$  is the experimentally determined diffusion coefficient. Based on this model, the seminal work by Epstein and Plesset [1], which describes successfully the  $t^{1/2}$  shrinkage dynamics of a spherical air bubble in an air-water solution, has been recently extended and the  $t^{1/2}$  scaling experimentally validated also for a liquid droplet (aniline or water) dissolving in a liquid-liquid (water-aniline or aniline-water) solution [2].

Fickian diffusion, however, is strictly limited to ideal mixtures and cannot hold for multiphase systems, even at thermodynamic equilibrium. A more general formulation for the mass flux can be found by means of nonequilibrium thermodynamics [3],  $\mathbf{j}_1 = -\nu_1\nabla\mu_1$ ,  $\mathbf{j}_2 = -\nu_2\nabla\mu_2$  or  $\mathbf{j} = -\nu\nabla\tilde{\mu}$ , where  $\mathbf{j} = \mathbf{j}_1 - \mathbf{j}_2$ ,  $\tilde{\mu} = \mu_1 - \mu_2$ ,  $\mu_1$  and  $\mu_2$  are the chemical potentials of the two components, and  $\nu_1$ ,  $\nu_2$ ,  $\nu$  are the mobility (or Onsager) coefficients. While the diffusivity  $D_0$  can be a constant for a binary system, the mobility coefficients are composition dependent [4]. For an ideal mixture or in the dilute limit, this formulation reduces to Fick's law. Following Cahn and Hillard [5], for a heterogeneous system, the local molar Gibbs free-energy  $g$  can be written as the sum of a local and a nonlocal contribution:  $g = g_{\text{loc}} + \frac{1}{2}a^2RT(\nabla\phi)^2$ , where  $a$  is the characteristic length scale of inhomogeneity [6] (different formulations for the free energy have also been developed [9]). Using a mobility coefficient of the

form  $\nu = \phi(1 - \phi)D_0$  and assuming the Flory-Huggins local free energy, Mauri *et al.* [7] proposed the net mass flux  $\mathbf{j} = -\phi(1 - \phi)D_0\nabla\tilde{\mu}$ , with  $\tilde{\mu} = \mu_0 + \log\frac{\phi}{1-\phi} + \Psi(1 - 2\phi) - a^2\nabla^2\phi$  where  $\Psi$  is the Margules parameter. As a result, we can write  $\mathbf{j} = -D_0\nabla\phi + \phi(1 - \phi)D_0(a^2\nabla\nabla^2\phi + 2\Psi\nabla\phi)$ ; in the dilute mixture limit,  $\phi(1 - \phi) \rightarrow 0$ , Fick's law is retrieved. The Mauri *et al.* [7] nonlinear diffusion equation ( $B$  model in the classification by Hohenberg and Halperin [10]) is able to describe a large variety of dynamical behaviors and therefore has been used to study different phenomena such as nucleation, spinodal decomposition of binary liquid alloys, mixing, and liquid drop coalescence and breakup [8].

In this Letter, we report experimental evidence on the behavior of a single liquid droplet immersed in a nonideal liquid-liquid mixture. We observe that as the droplet dissolves its radius shrinks linearly with time, i.e.  $R(t) \sim -\alpha t$ , and not as  $R(t) \sim -\alpha t^{1/2}$  as Fickian diffusion as well as the nonlinear  $B$  model would predict if convection is neglected. We will show that the scaling law we observe is an effect of the importance of hydrodynamic convection effects during mass transfer [11], generated by the droplet self-propelling around while dissolving [12], caused by Korteweg forces [7,13].

In our experiments, we use binary liquid mixtures of acetone and hexadecane because they are partially miscible (Fig. 1) and have density differences lower than 0.1% and negligible excess volume at all compositions; therefore, buoyancy effects can be neglected. At 20 °C (Fig. 1), the stable equilibrium state is two-phase; i.e., the mixture is separated into phase  $\mathcal{A}$  (25% acetone, 75% hexadecane by volume) and  $\mathcal{B}$  (80% acetone, 20% hexadecane by volume). To allow visualization, 50 ppm of crystal violet (that preferentially mixes with acetone) are added. Crystal violet is a cationic emulsifier, but at such low concentration it has no effect on the solubility limits [13]. We inject a droplet of either pure hexadecane  $\mathcal{H}$  or phase  $\mathcal{A}$  into phase  $\mathcal{B}$  and observe its time evolution.

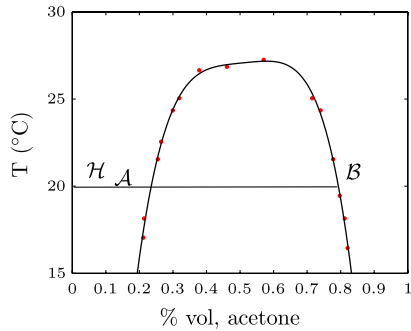


FIG. 1 (color online). Phase diagram for acetone-hexadecane mixtures, Ref. [20]. Continuous line: solubility limit curve.

To inject droplets, we take advantage of microfluidics and we fabricate poly-dimethyl-siloxane (PDMS) devices using soft lithography [14]. Droplets are produced by the well-known flow focusing geometry [15] shown in Fig. 2. Through the side branches, we inject a mixture with composition  $\mathcal{B}$  which in the downstream channel forms the continuous phase, while in the central branch we slowly inject either pure hexadecane or a mixture with composition  $\mathcal{A}$ . The channel is  $50 \mu\text{m}$  wide and  $15 \mu\text{m}$  high. Both liquids are pumped from pressurized containers, whose pressure is controlled by ACSI-100LR precision valves. Although hexadecane swells PDMS, we do not observe changes in our setup during the experiments—as already noted in [16]. Once a droplet is obtained, both streams are stopped and images are recorded at 60 fps using a CCD camera mounted on a Zeiss (Axiovert 200 M) microscope. Images are postprocessed with standard and *ad hoc* software written in Matlab© to identify the pure hexadecane region of the droplet and replace it by the best fitting circle, so its radius and center location are recorded. Injected droplets have an initial radius  $\bar{r}_0 \sim 20 \mu\text{m}$  and we follow their evolution down to  $\bar{r} \sim 2 \mu\text{m}$ .

Based on energy considerations and taking into account the contact angles, it can be shown that in our experiments the droplets are cylindrical in shape, with both cylinder bases in permanent contact with the top and bottom channel walls. As shown in experimental validations of the EP theory [17], the fact that a droplet is attached to an impermeable wall does not affect its dissolution dynamics.

As expected, when droplets are of composition  $\mathcal{A}$ , nothing happens, the droplet neither shrinks nor moves around, because phase  $\mathcal{A}$  is in mutual thermodynamic equilibrium with the background phase  $\mathcal{B}$ . Even though this is a trivial result, it was necessary to show that no spurious effects (such as thermocapillary or buoyancy) are present.

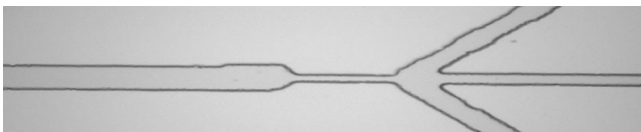


FIG. 2. In-line flow focusing device used to generate droplets.

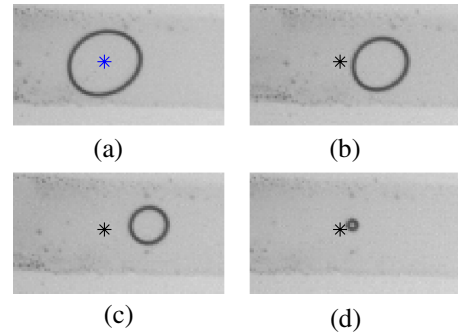


FIG. 3 (color online). A few snapshots of the dissolving droplet. The circle is obtained by image postprocessing and identifies the pure hexadecane region of the droplet. (a)  $t = 0$  s, (b)  $t = 1.1$  s, (c)  $t = 2.3$  s, (d)  $t = 3.9$  s. The \* indicates the initial droplet ( $t = 0$  s) center.

More interesting is the injection of pure hexadecane into phase  $\mathcal{B}$ , since they are not in mutual equilibrium. A few snapshots are shown in Fig. 3. The time evolution of the drop radius  $\bar{r}(t)$  is shown in Fig. 4 for two of the 32 different repetitions of the same experiment we analyzed. By fitting a power law of the form  $\bar{r}(t) = \bar{r}_0 - \alpha t^\beta$ , we find  $\beta = 0.996 \pm 0.07$ , showing that shrinkage is linear in time. The shrinkage rate  $d\bar{r}/dt = -\alpha$  is in the range  $3 \mu\text{m/s}$  to  $8 \mu\text{m/s}$  and remains nearly constant while the droplet radius changes over one order of magnitude. Our main experimental result is that the droplet self-propels around and its radius shrinks with a  $t^1$  scaling, instead of the typical  $t^{1/2}$  fingerprint of a purely diffusive process (linear or nonlinear diffusion equation neglecting convective terms). The  $t^1$  scaling can only be explained as a consequence of hydrodynamic convective effects due to the motion of the droplet [11,13,18]. Since no flow nor pressure, temperature, nor concentration gradients are present in the background phase  $\mathcal{B}$ , the droplet motion must be self-generated by dissolution dynamics. While numerical simulations of a droplet out of thermodynamic equilibrium have shown that self-propelled motion is possible even in an isotropic background concentration field

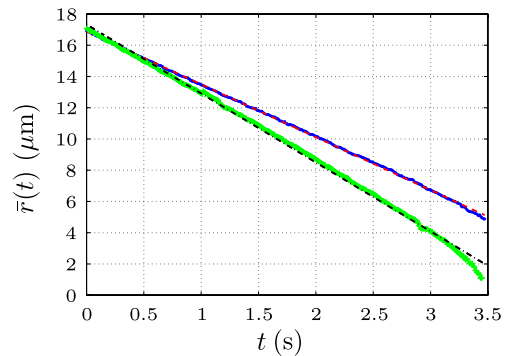


FIG. 4 (color online). Time evolution of the droplet radius  $\bar{r}(t)$  for two repetitions of the experiment. Fitting by a linear relation  $\bar{r}(t) = \bar{r}_0 - \alpha t$  is good. For the two cases  $R^2 = 0.98$  and  $R^2 = 0.99$ .

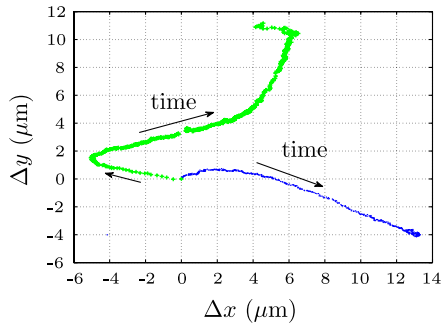


FIG. 5 (color online). Droplet center at different instants of time for the two dissolving droplets of Fig. 4. Initial position is set at (0,0); time increases along the arrow.

[19], detailed experimental evidence has not been shown before [12].

By following the center of a nonequilibrium droplet (Fig. 3), we can generate a trace of the path that it follows during dissolution. A trace of two representative degradation pathways is shown in Fig. 5. Differently from the numerical simulations by Vladimirova *et al.* [19], our droplets do not move isotropically, but preferentially along the channel axis direction. The ratio of the transverse to axial components of velocity is about 1/10, due to the side wall which modifies the details of droplet life and makes the mass transfer non isotropic.

When a droplet of pure hexadecane is placed in a  $\mathcal{B}$ -phase background, it alters the local composition away from stable equilibrium into the metastable and then the unstable equilibrium region under the spinodal curve, where phase  $\mathcal{A}$  is rapidly formed through a thin, but finite thickness, phase  $\mathcal{A}$ -phase  $\mathcal{B}$  interface. What we see in our experiments is, therefore, a complex transient bringing the system through nonequilibrium states to a new stable equilibrium state where a larger droplet of phase  $\mathcal{A}$  is in mutual equilibrium with the  $\mathcal{B}$  phase background. For brevity reasons and because the image postprocessing required to distinguish phase  $\mathcal{A}$  from phase  $\mathcal{B}$  introduces more uncertainty than to distinguish pure hexadecane, we present and discuss here only the sharp data on the pure hexadecane inner region of the droplet, which shrinks linearly with time. The growth of the less sharp interface (between phase  $\mathcal{A}$  and phase  $\mathcal{B}$ ) is also linear in time (data not shown), in confirmation of our main observation. For the composition in the droplet to move from pure hexadecane towards phase  $\mathcal{A}$ , it must adsorb acetone and desorb hexadecane. It does so by diffusive mixing with phase  $\mathcal{A}$  as soon as phase  $\mathcal{A}$  is formed by phase change from phase  $\mathcal{B}$ . Phase change from  $\mathcal{B}$  to  $\mathcal{A}$  is a rapid process (except for its triggering stage across the metastable region). Diffusive mixing of  $\mathcal{A}$  with the hexadecane-rich zone would instead be a slow process in the absence of convective motion. The observed motion produces instead higher local concentration gradients thus effectively speeding up the diffusive mixing. We believe that the self-generated motion is driven by Korteweg forces ( $\mathbf{F}_\phi =$

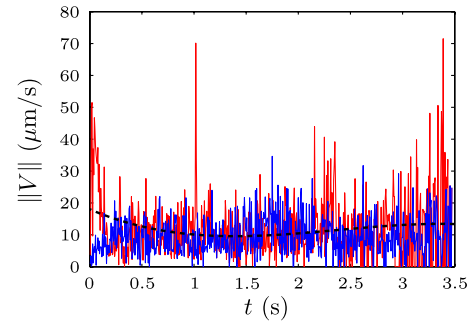


FIG. 6 (color online). Droplet speed  $\|V\|$  for two repetitions of the experiment (same as in Fig. 4). Despite the noise, in both instances the droplet speed is of order  $15 \mu\text{m/s}$ , throughout the dissolving interval.

$\tilde{\mu}\nabla\phi$  [19]) during the rapid phase-change part of the process (through the nonequilibrium region of the phase diagram). Even though the velocity of the droplet is relatively small ( $15\text{--}25 \mu\text{m/s}$ ), such a motion modifies the mass transfer.

Our results differ from those recently obtained by Duncan and Needham [2] for aniline droplets dissolving in water, which are consistent with the Epstein and Plesset (1950) solution of the diffusion equation combined with the equilibrium hypothesis; i.e., the droplet radius shrinks as  $\sim t^{1/2}$ . The difference relies in the fact that water and aniline at room temperature are totally miscible while, in our case, acetone and hexadecane are only partially miscible and the system, to reach equilibrium, has to pass through a series of nonequilibrium states across the miscibility gap, where even the local equilibrium hypothesis breaks down.

The instantaneous droplet speed  $\|V\|$  is represented as a function of time in Fig. 6, showing that it is almost independent of droplet size. This was anticipated using an order of magnitude reasoning by equating the driving and the viscous force, see Molin [8], as well as by numerical simulations [19]. The droplet dissolution dynamics is increasingly dominated by convective effects, which greatly enhance diffusion by producing higher local concentration gradients. The speeds we measured (in the range  $15\text{--}25 \mu\text{m/s}$ ) are in agreement with the values reported in [19].

In summary, in this Letter we have shown that when a liquid droplet is placed in a uniform liquid-liquid solution, Fick's law may not be sufficient to describe its dissolution. For partially miscible liquids, if the droplet to dissolve requires a phase change across the miscibility gap, the coupling between mass and momentum transfer known as Korteweg forces induces a vigorous self-propelled motion of the droplet. This motion results in a convective effect, which greatly enhances diffusion and changes the scaling of the droplet dissolution from  $t^{1/2}$  (typical of nonconvective Fickian as well as nonlinear diffusion) to  $t^1$ .

We thank Prof. H. A. Stone for pointing us to EP theory. We acknowledge Prof. R. Mauri and Prof. A. M. Lezzi for

helpful discussions. Work done in part under the UniBS-MIT-MechE faculty exchange Program co-sponsored by the CARIPLO Foundation, Italy under Grant No. 2008-2290.

\*pietro.poesio@ing.unibs.it

- [1] P. S. Epstein and M. S. Plesset, *J. Chem. Phys.* **18**, 1505 (1950).
- [2] P. B. Duncan and D. Needham, *Langmuir* **20**, 2567 (2004); **22**, 4190 (2006).
- [3] S. R. DeGroot and P. Mazur, *Non-Equilibrium Thermodynamics* (Dover Publications, Amsterdam, 1962); S. Kjelstrup and D. Bedeaux, *Non-Equilibrium Thermodynamics of Heterogeneous Systems* (World Scientific, Singapore, 2008); J. Lowengrub and L. Truskinovsky, *Proc. R. Soc. A* **454**, 2617 (1998).
- [4] A careful analysis of the effect of a composition-dependent mobility can be found in the following references: S. Puri, A. J. Bray, and J. Lebowitz, *Phys. Rev. E* **56**, 758 (1997); J. S. Langer, M. Baron, and H. D. Miller, *Phys. Rev. A* **11**, 1417 (1975); K. Kitahara and M. Imada, *Prog. Theor. Phys. Suppl.* **64**, 65 (1978); F. Corberi, M. Nicodemi, M. Piccioni, and A. Coniglio, *Phys. Rev. Lett.* **83**, 5054 (1999).
- [5] J. W. Cahn and J. E. Hillard, *J. Chem. Phys.* **28**, 258 (1958); J. W. Cahn, *J. Chem. Phys.* **30**, 1121 (1959); J. W. Cahn and J. E. Hillard, *J. Chem. Phys.* **31**, 688 (1959).
- [6] Discussions on nonlocal formulations of the free energy are far from being settled. Mauri *et al.* [7,8] and many others assumed that the nonlocality of the free energy is represented by the term  $a^2(\nabla\phi)^2$  alone—Landau-Ginzburg potential—neglecting higher order terms.
- [7] R. Mauri, R. Shinnar, and G. Triantafyllou, *Phys. Rev. E* **53**, 2613 (1996); N. Vladimirova, A. Malagoli, and R. Mauri, *Phys. Rev. E* **58**, 7691 (1998).
- [8] N. Vladimirova, A. Malagoli, and R. Mauri, *Chem. Eng. Sci.* **55**, 6109 (2000); A. G. Lamorgese and R. Mauri, *Phys. Fluids* **17**, 034107 (2005); **18**, 044107 (2006); N. Vladimirova and R. Mauri, *Chem. Eng. Sci.* **59**, 2065 (2004); D. Molin, Ph.D. thesis, Università di Pisa (Italy), 2008 (unpublished).
- [9] Landau-type free energy  $g_{\text{loc}}/RT = -\frac{1}{2}\phi^2 + \frac{1}{4}\phi^4$  is often used, see M. Conti, B. Meerson, and P. V. Sasorov, *Phys. Rev. Lett.* **80**, 4693 (1998), and references therein; T. Araki and H. Tanaka, *Phys. Rev. Lett.* **93**, 015702 (2004) proposed a formulation based on two order parameters to study phase separation of an isotropic liquid and a liquid crystal; V. E. Badalassi, H. D. Ceniceros, and S. Banerjee, *J. Comput. Phys.* **190**, 371 (2003) proposed a double well potential of the form  $g_{\text{loc}}/RT = c_1(\phi - c_2)^2(\phi + c_2)^2$  to study drop deformation in a shear flow; Mauri *et al.* [7,8] and E. B. Nauman and D. Q. He, *Chem. Eng. Sci.* **56**, 1999 (2001) used a Flory-Huggins potential to describe spinodal decomposition.
- [10] P. C. Hohenberg and B. I. Halperin, *Rev. Mod. Phys.* **49**, 435 (1977); A. J. Bray, *Phil. Trans. R. Soc. A* **361**, 781 (2003).
- [11] H. Furukawa, *Phys. Rev. E* **55**, 1150 (1997); E. Siggia, *Phys. Rev. A* **20**, 595 (1979); N. C. Wang and C. M. Knobler, *Phys. Rev. A* **24**, 3205 (1981).
- [12] The motion of droplets out of thermodynamic equilibrium has been observed experimentally during spinodal decomposition of low viscosity binary liquid alloys [13]. Self-propelled motion of a single droplet has been observed also elsewhere. O. Kogi, K. Yuya, H. Kim, and N. Kitamura, *Langmuir* **17**, 7456 (2001) studied the behavior of a single micrometer-sized oil droplet that forms at the end of a capillary tube in water; self-propulsion of a single nematic droplet was observed by S. Thakur, P. S. Kumar, N. Madhusudam, and P. A. Pullurkat, *Phys. Rev. Lett.* **97**, 115701 (2006); in that case, a surface flow, induced by the gradient in the concentration of the dopant expelled by the growing drops, provides the propelling force; Recently, C. M. Bates, F. Stevens, S. C. Langford, and J. T. Dickinson, *Langmuir* **24**, 7193 (2008) observed fast dissolution of alcohol droplets in water and self-propelled motion driven by surface tension gradients.
- [13] P. Poesio, G. Cominardi, A. M. Lezzi, R. Mauri, and G. P. Beretta, *Phys. Rev. E* **74**, 011507 (2006); P. Poesio, A. M. Lezzi, and G. P. Beretta, *Phys. Rev. E* **75**, 066306 (2007).
- [14] T. Thorsen, S. J. Maerkl, and S. R. Quake, *Science* **298**, 580 (2002); H. Becker and L. E. Locascio, *Talanta* **56**, 267 (2002); G. M. Whitesides, E. Ostuni, S. Takayama, X. Jiang, and D. E. Inberg, *Annu. Rev. Biomed. Eng.* **3**, 335 (2001); E. Verpoorte and N. F. De Rooji, *Proc. IEEE* **91**, 930 (2003).
- [15] S. L. Anna, N. Bontoux, and H. A. Stone, *Appl. Phys. Lett.* **82**, 364 (2003); A. M. Ganan-Calvo and J. M. Gordillo, *Phys. Rev. Lett.* **87**, 274501 (2001).
- [16] D. R. Link, S. L. Anna, D. A. Weitz, and H. A. Stone, *Phys. Rev. Lett.* **92**, 054503 (2004).
- [17] L. Leibermann, *J. Appl. Phys.* **28**, 205 (1957); D. M. J. P. Manley, *J. Appl. Phys.* **11**, 28 (1960); C. A. Ward, A. S. Tucker, and C. W. So, *J. Chem. Phys.* **83**, 543 (1978); D. L. Wisse and G. Houghton, *Chem. Eng. Sci.* **23**, 1211 (1968); M. A. Borden and M. L. Longo, *Langmuir* **18**, 9225 (2002); S. Kentish, J. Lee, M. Davidson, and M. Ashokkumar, *Chem. Eng. Sci.* **61**, 7697 (2006).
- [18] The mass balance for a droplet of volume  $V$  and surface area  $A$  is  $\rho dV/dt = -JA$  where  $J$  is the net average mass flux. Whether the droplet is spherical or cylindrical with impermeable bases, this yields  $d\bar{r}/dt = -J/\rho$ . Classical correlations between Sherwood, Péclet, and Schmidt numbers [see R. Clift, J. R. Grace, and M. E. Weber, *Bubble, Drops, and Particles* (Dover, New York, 1978)] do not account for flow field effects caused by Korteweg stresses and, therefore, are not readily applicable here to estimate  $J/\rho$ . However, the diffuse interface formulation proposed by Mauri and co-workers [7,8] accounts for convection generated by Korteweg forces, yielding  $J/\rho = D[2\Psi\bar{\phi}(1 - \bar{\phi}) - 1]\Delta\phi/\ell$  with  $\ell$  the interface thickness. Combined with the observation that  $J/\rho = -d\bar{r}/dt$  remains constant for our droplet, this theory implies the reasonable conclusion that  $\Delta\phi/\ell$  remains constant during dissolution.
- [19] N. Vladimirova, A. Malagoli, and R. Mauri, *Phys. Rev. E* **60**, 2037 (1999); D. Molin, R. Mauri, and V. Tricoli, *Langmuir* **23**, 7459 (2007).
- [20] E. A. Macedo and P. Rasmussen, *Liquid-Liquid Equilibrium Data Collection. Supplement 1*, Chemistry Data Series Vol. V (DECHEMA, Frankfurt, 1987), Part 4, p. 52.